Integrative and Comparative Biology

Integrative and Comparative Biology, volume 0, number 0, pp. 1–12
https://doi.org/10.1093/icb/icac042

Society for Integrative and Comparative Biology

SYMPOSIUM

Bat Dentitions: A Model System for Studies at the Interface of Development, Biomechanics, and Evolution

Sharlene E. Santana [*,†,1,2], David M. Grossnickle [*,2], Alexa Sadier [‡,2], Edward Patterson [*] and Karen E. Sears [‡]

[*]Department of Biology, University of Washington, Seattle, WA 98195, USA; [†]Burke Museum of Natural History and Culture, University of Washington, Seattle, WA 98195, USA; [‡]Department of Ecology and Evolutionary Biology, University of California Los Angeles, Los Angeles, CA 94611, USA

[2]joint first authors

From the symposium "Integrating ecology and biomechanics to investigate patterns of phenotypic diversity: Evolution, development, and functional traits" presented at the annual meeting of the Society for Integrative and Comparative Biology virtual annual meeting, January 3–February 28, 2022.

[1]E-mail: ssantana@uw.edu

Synopsis The evolution of complex dentitions in mammals was a major innovation that facilitated the expansion into new dietary niches, which imposed selection for tight form–function relationships. Teeth allow mammals to ingest and process food items by applying forces produced by a third-class lever system composed by the jaw adductors, the cranium, and the mandible. Physical laws determine changes in jaw adductor (biting) forces at different bite point locations along the mandible (outlever), thus, individual teeth are expected to experience different mechanical regimes during feeding. If the mammal dentition exhibits functional adaptations to mandible feeding biomechanics, then teeth are expected to have evolved to develop mechanically advantageous sizes, shapes, and positions. Here, we present bats as a model system to test this hypothesis and, more generally, for integrative studies of mammal dental diversity. We combine a field-collected dataset of bite forces along the tooth row with data on dental and mandible morphology across 30 bat species. We (1) describe, for the first time, bite force trends along the tooth row of bats; (2) use phylogenetic comparative methods to investigate relationships among bite force patterns, tooth, and mandible morphology; and (3) hypothesize how these biting mechanics patterns may relate to the developmental processes controlling tooth formation. We find that bite force variation along the tooth row is consistent with predictions from lever mechanics models, with most species having the greatest bite force at the first lower molar. The cross-sectional shape of the mandible body is strongly associated with the position of maximum bite force along the tooth row, likely reflecting mandibular adaptations to varying stress patterns among species. Further, dental dietary adaptations seem to be related to bite force variation along molariform teeth, with insectivorous species exhibiting greater bite force more anteriorly, narrower teeth and mandibles, and frugivores/omnivores showing greater bite force more posteriorly, wider teeth and mandibles. As these craniodental traits are linked through development, dietary specialization appears to have shaped intrinsic mechanisms controlling traits relevant to feeding performance.

Introduction

The diversification of mammals was largely facilitated by the evolution of complex dentitions that enabled expansion into a wide array of dietary niches (Hunter and Jernvall 1995; Evans et al. 2007; Martin et al. 2020; Grossnickle et al. 2022). The dental arcade of mammals includes different types of teeth with functionally specialized morphologies—incisors for grasping, cutting, and grooming, canines for piercing and stabbing, and premolars and molars for cutting and grinding. The evolution of complex molariform teeth, in particular, was a key step in mammal evolution (Patterson 1956; Crompton 1971; Luo 2007; Schultz and Martin 2014; Martin et al. 2020). From an ancestral tribosphenic mo-

Advance Access publication May 16, 2022

lar morphology that enabled shearing and grinding, mammal molars diversified dramatically along multiple axes (e.g., overall shape, cusp number and shape, crown height), leading to an exceptionally high morphological diversity that is tightly associated with the physical demands imposed by diverse diets (e.g., Evans et al. 2007; Pineda-Munoz et al. 2016).

From a biomechanical and ecological perspective, diversity in dental functional morphology in mammals could be related to differences in the mechanical demands experienced by teeth in relation to their position along the mandible, that is, the forces each tooth applies during biting on food items. In mammals that use orthal-dominated chewing movements (e.g., chiropterans, carnivorans), the feeding apparatus is a lever system in which the bite force at a given tooth is the result of the forces generated by the jaw adductors—which create a moment about the mandible joint—divided by the outlever, or the distance between the mandible joint and the biting tooth (Fig. 1A). If all other variables are kept constant, the outlever will be shortest in the most posteriorly positioned tooth (i.e., the ultimate molar), and thus the ultimate molar is expected to apply the greatest bite force among all teeth. We refer to this as the "unconstrained model." A more nuanced view of these patterns was proposed by Greaves (1978, 2002) and Spencer (1995, 1999), who further defined three bite force regions based on a constrained bite force model that takes into account the potential for dislocation of the mandible on the balancing side at more posterior bite points (Fig. 1B and C). Under this "constrained model," bite force would be greatest somewhere along the molariform dentition and then decrease in the more posterior region of the mandible. While these models have not been validated experimentally in the majority of mammal species (but see Spencer 1998), it is widely accepted that mammals produce greater bite forces in posterior regions of the tooth row. It follows that, because bite force is expected to be under selection to match the physical demands of dietary items (e.g., Herrel et al. 2005; Christiansen and Wroe 2007; Dumont et al. 2012), biting mechanics could partly explain the morphological diversity of teeth —especially molars—in mammals.

An examination of extrinsic factors can only provide a partial explanation for the diversity of form and function in mammal teeth; much still needs to be understood about how these interact with intrinsic factors to shape dental diversity in mammals. As stated above, the bite force at each tooth depends on the tooth's morphology and its location within the mandible. Both of these parameters are determined during development by processes that define precise position of teeth in the mandible (Kavanagh et al. 2007; Sadier et al. 2021) and tooth shape (Tucker and Sharpe 2004). However, little is known about how these developmental processes are regulated, for several reasons. For instance, studies of mammalian tooth development are limited primarily to mice and focus on molars. These studies have revealed that tooth position is determined through activation/inhibition mechanisms that regulate the successive apparition of teeth (Kavanagh et al. 2007), and that molar development involves two main tissues—the dental epithelium and the underlying mesenchyme—that cross-talk during all stages of tooth development (i.e., bud, cap, and bell) (reviewed in Catón and Tucker 2009). But, because mice have highly derived cranial morphologies and dentitions (e.g., loss of canines, ever growing incisors) associated with relatively unique masticatory functions (e.g., incisor gnawing and anteriorly-directed molar chewing; Hiiemäe and Ardran 1968), there is limited knowledge about the development of non-molar tooth classes, including its relation to biting mechanics in mammals. Further, while there is evidence that the early patterning of the mandible is driven by a so-called homeobox-code model, which would divide the mandible into territories responsible for tooth class determination prior to tooth bud development (reviewed in Catón and Tucker 2009; Wakamatsu et al. 2019), little is known about how the mechanisms by which the homeobox code could influence tooth initiation and morphogenesis. Moreover, the idea of a homeobox-code model has recently been challenged by studies of a lizard that also exhibits a heterodont dentition (*Pogona*; Salomies et al. 2021). While shifts in gene expression patterns have been observed between tooth classes at the bud, cap, and bell stages, the impact of these differences on tooth class identity and morphogenesis remains unclear (Moustakas et al. 2011). Thus, the field of mammalian evolution is in need of a system in which to study these topics in a comparative context. Ideally, this would be a group of species that exhibit a complete dentition, a broad diversity of dental morphologies and diet types, and different physical demands associated with these diets.

Here, we present bats as a model for integrative studies of dental diversity in mammals. Bats have exceptional diversity in terms of number of species (over 1400 species), dietary ecology, and craniodental morphology (Arbour et al. 2019; Simmons and Cirranello 2022). This diversity is particularly high in some groups like the superfamily noctilionoidea, which includes seven families and over 200 species and spans the greatest dietary diversity of all bats—ranging from insectivory, to plant-based diets (nectarivory and frugivory), carnivory, omnivory, and even blood feeding (Fig. 2). Along with dietary diversity, bats exhibit exceptional variation in tooth number and molar morphol-

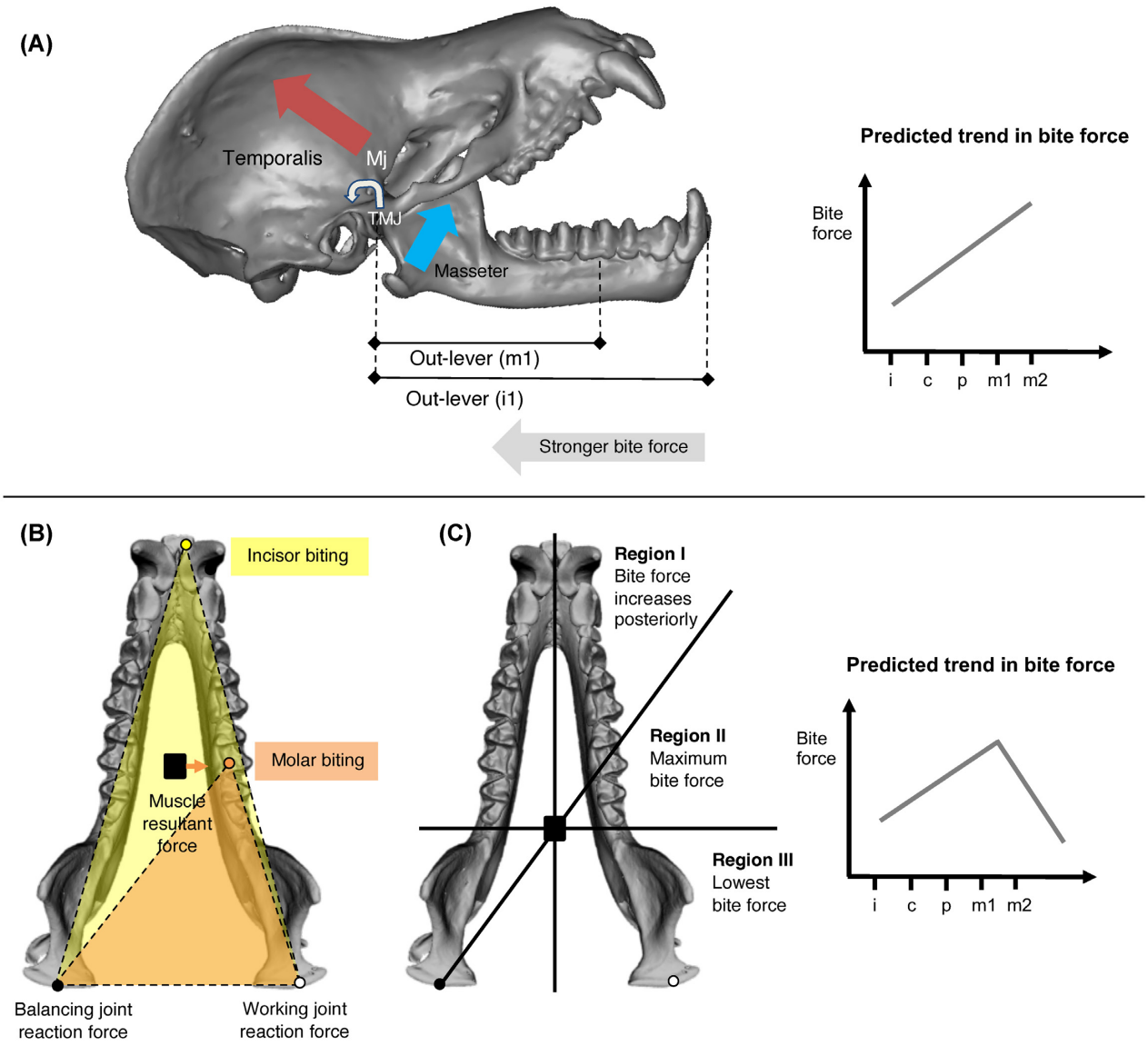

Fig. 1 Two models of bite force variation along the tooth row. **A)** in an unconstrained model, bite force is proportional to the moment (Mj) about the jaw joint (temporomandibular joint, TMJ), which can be calculated as the sum of the moments about the TMJ produced by the jaw adductor muscles (temporalis and masseter) divided by the outlever (distance between the bite point and the TMJ). Bite force is predicted to increase at more posterior bite points along the tooth row. **B)** in a constrained model proposed by Greaves (1978, 2002) and Spencer (1995, 1999), a triangle of support (shaded area) is defined by the bite point and the working and balancing jaw joint reaction forces; a midline mandible muscle resultant force passes through this triangle during more anterior biting, and has to be repositioned toward the working side of the mandible to avoid tension in the jaw joint during more posterior biting. **C)** based on perpendicular and oblique planes drawn based on the position of the mandible muscle resultant force, Greaves (1978, 2002) proposed three bite force regions: Region I, in which bite force increases posteriorly as in the unconstrained model; Region II, the region of maximum bite force; and Region III, with the lowest bite force because biting would be associated with dislocation of the balancing side jaw joint. Bite force is predicted to increase, reach a maximum, and then decrease posteriorly along the mandible.

ogy (Freeman 1998). Using a comparative dataset spanning 30 species and five families, we explore the hypothesis that bat molars exhibit functional adaptations to mandible feeding biomechanics and have evolved to develop mechanically advantageous dimensions and positions along the mandible. We will specifically focus on the following questions: (1) How does bite force vary along the tooth row? (2) What is the relationship between the point of maximum bite force along the tooth row, tooth, and mandible morphology? And (3) how could bite force–morphology relationships relate to the developmental processes controlling tooth formation? Past studies have illuminated numerous aspects of bat skull biomechanics through modeling approaches (e.g.,

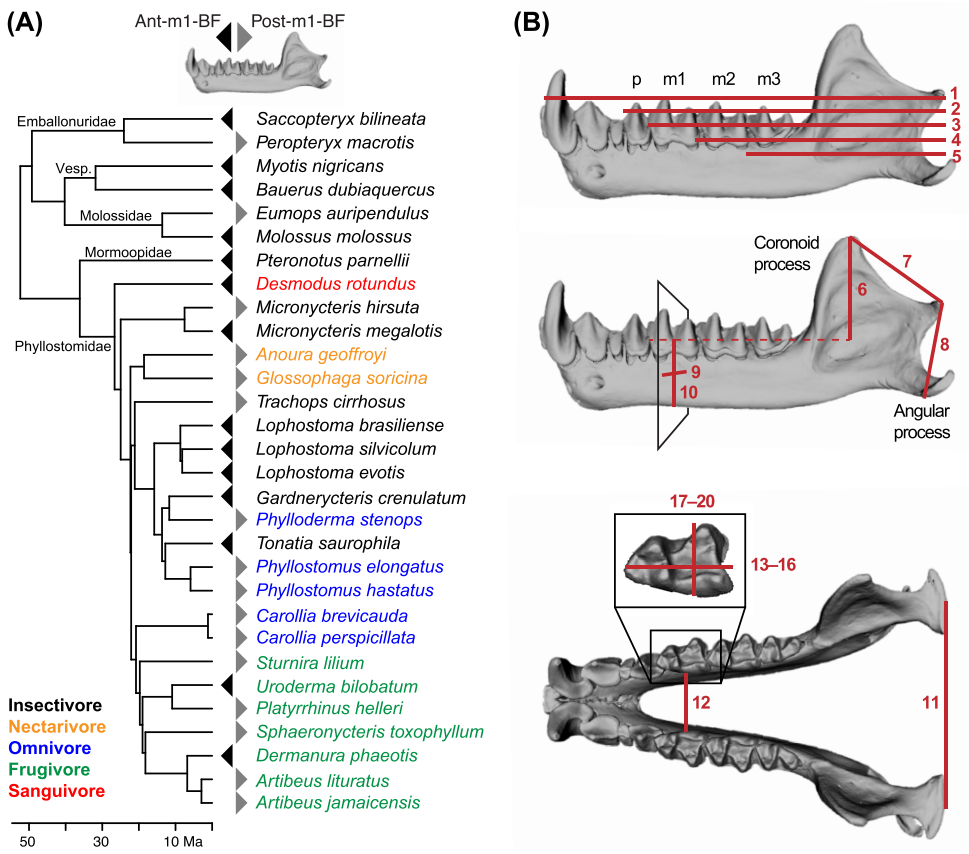

Fig. 2 A) Phylogeny (pruned from Upham et al. 2019) showing the species included in this study, their primary diets, and the bite force group to which they belong (ant-m1-BF: anterior bite force; post-m1-BF: posterior bite force, see text for descriptions). **B)** Measurements included in the analyses relating bite force trends with mandible and tooth morphology: (1) length of the mandible, measured from the anterior margin of the mandibular synthesis to the posterior margin of the condylar process, parallel to the molar row; (2) ultimate premolar to the condylar process; (3) first lower molar (m1) to the condylar process; (4) second lower molar to the condylar process; (5) third lower molar to the condylar process; (6) height of the coronoid process above the dorsal margin of the mandible body (dashed line); (7) coronoid process (dorsal margin) to the mandible joint (TMJ), which approximates the inlever length of the temporalis muscle; (8) angular process (ventral margin) to the mandible joint, which approximates the inlever lengths of the masseter and medial pterygoid muscles; (9) width of the mandible body at m1, measured at the mid-point of the length of m1; (10) height of the mandible body at m1, measured at the mid-point of the length of m1; (11) width of the mandible at the mandible joints, measured as the distance between mandible joints (mid-points of the condylar process); (12) width of the mandible at m1, measured as the distance between the medial margins of the left and right m1; (13–16) maximum lengths of the ultimate premolar and molars; (17–20) maximum widths of the ultimate premolar and molars.

Dumont et al. 2005; Santana et al. 2010, 2012; Santana 2016). However, empirical data about how bite force varies along the tooth row is lacking, preventing a full understanding of the relationship among biting mechanics, tooth development, and morphology. By integrating morphological and performance data with information about tooth development, we begin to shed light on how the interaction between intrinsic and extrinsic factors could have shaped dental diversity in bats.

Methods

Bite force along the tooth row

We evaluated how bite force changes along the tooth row, and if these trends match those predicted by models of bite force production (Fig. 1). We considered that a gradual increase in bite force posteriorly along the tooth row would be consistent with the unconstrained model of bite force (Fig. 1A), whereas an increase in bite force at the molariform teeth followed by a decrease in more posterior regions of the mandible would be consistent with the constrained model (Fig. 1B). To test these predictions, we measured *in vivo* bite forces from 30 bat species across five families (Emballonuridae, Molossidae, Mormoopidae, Phyllostomidae, and Vespertilionidae; 81 individuals, $n = 1–9$ per species; Fig. 2; Supplementary Table 1) in localities in Venezuela and Belize. We used mist nets to capture bats, and selected only adult males and adult, non-pregnant, non-lactating females for this study. Shortly after capture, we measured

each bats' voluntary bite force using a piezoelectric force transducer (Kistler, type 9203, range ± 500 *N*, accuracy 0.01–0.1 *N*; Amherst, NY, USA) mounted between two stainless steel plates (e.g., Herrel et al. 1999; Santana and Dumont 2009), and attached to a handheld charge amplifier (Kistler, type 5995, Amherst, NY, USA). The plates had a 1 mm wide tip that allowed us to measure bite force at specific teeth. We covered plate tips in medical tape to provide a non-skid surface and to protect the bats from injury during biting. We measured bite force on one side of the mandible at five points along the tooth row: incisors (i), canine (c), premolars (p), first molar (m1), and second molar (m2). Very few species were large enough to accommodate the plates at the third molar (m3) or more posteriorly (r3), and most bats were not willing to bite the plates using this region of the mandible. In all trials, we adjusted the distance between the bite plates for each individual to accommodate an intermediate gape angle of approximately 30° (Santana 2016), measured between the corner of the mouth and the plane defined by the teeth in contact with the meter. We recorded at least five measurements at each biting point for each bat, allowing bats to rest between measurements. All procedures complied with Institutional Animal Care and Use protocols (UMass 26–10–06; UW 4307–01). For statistical analyses, we selected the maximum value across measurements at each bite point per bat and averaged these values across individuals per species.

Mandible and tooth morphology

To identify which mandible and tooth morphology traits relate to the observed patterns of bite force along the tooth row, we generated 3D models of skulls from either (1) micro computed tomography (μCT) scans (Skyscan 1172 μCT scanner, Bruker, Belgium) of specimens we collected in the field or sourced from museums or (2) downloaded from the online repository MorphoSource (www.morphosource.org; Supplementary Table 1). From each mandible model, we took 12 measurements (Fig. 2) that reflect mechanically important traits, including (1) linear measurements that capture the position (out-levers) of different tooth types along the mandible; (2) the height of the coronoid process, which influences the moment generated by the temporalis muscle about the jaw joint; and (3) distances from the condyle to the angular or coronoid process, which are proxies for the temporalis and masseter in-levers, respectively, and proportional to their moments about the jaw joint. We also measured the width and height of the mandible and calculated their ratio, which should reflect the overall mandible body shape and resistance to dorsoventral loads like those produced during orthal biting and chewing (Therrien 2005). We also took eight dental measurements, including the lengths and widths of the lower ultimate premolar (most commonly p3) and three molars (m1–m3); ultimate premolars were selected to maintain the same number of measurements across species in our analyses, because the number of premolars varied among species in our sample. *Dermanura phaeotis* lacks an m3, and *Desmodus rotundus* lacks an m2 and m3, and thus, we did not collect eight measurements for these two species. All measurements are shown and described in Fig. 2.

Statistical analyses

Prior to analyses, we standardized each tooth-specific bite force value by dividing it by the maximum bite force at any tooth along the tooth row. To minimize the influence of size on the mandible and dental measurements, we either converted measurements to functional ratios (e.g., cross-sectional shape of the mandible body) or divided measurements by the geometric mean of several mandible measurements (as a proxy for mandible size). Tooth areas in the occlusal plane (lengths multiplied by widths) were standardized by dividing by the total area of the measured teeth (ultimate premolar through ultimate molar). This resulted in 19 size-corrected traits that we then used in subsequent comparative analyses. The mandible geometric mean was calculated using mandible length, coronoid-to-mandible-joint distance, angle-to-mandible-joint distance, mandible body height, and mandible body width (measurements 1, 7, 8, 9, and 10 in Fig. 2). The single vampire bat in our sample, *Desmodus rotundus*, is a major morphological and functional outlier with unique features (e.g., considerably reduced check teeth and a lack of posterior molars), and thus we chose to exclude it from comparative analyses.

For comparative analyses, we used a maximum clade credibility (MCC) tree based on 1000 phylogenetic trees from the "completed trees" sample in Upham et al. (2019). The MCC tree was generated using *TreeAnnotator* (Drummond et al. 2012), and the tree was pruned to the 29 species in our sample.

We used two types of analyses to examine the relationship between the position of greatest bite force along the tooth row and the size-corrected mandibular and dental traits. First, we classified species into one of two groups based on the position of maximum bite force relative to the first lower molar (ant-m1-BF or post-m1-BF, see Results for details on how these groups were defined) and then used phylogenetic ANOVAs (pANOVAs) with phylogenetic generalized least-squares (PGLS) regression models to test for differences in morphological traits between these

two groups. Second, we measured the distance from the tooth with maximum bite force to the mandibular condyle and divided this measurement by mandible length. For example, if the m1 had the maximum bite force of any cheek tooth, then measurement #3 (m1 to condyle distance; Fig. 2B) was divided by measurement #1 (mandible length). We then used these ratios as response variables in PGLS regressions with morphological measurements (Fig. 2) as predictors. PGLS analyses were performed using the *pgls* function in the *caper* R package (Orme et al. 2018). A key difference between these two approaches is the reference for determining the position of the maximum bite force; for the first method, maximum bite force position is *relative to the m1* (either anterior to m1 or posterior to m1), and for the second method, maximum bite force position is *relative to mandible length*.

Results and discussion

How does bite force vary along the tooth row?

We find that most bat species show a similar pattern in bite forces along the tooth row. Starting at the incisors, most species exhibit a decrease in bite force at the canines, followed by an increase at the premolars, which continues until reaching a maximum at the molars (m1 or m2; Fig. 3 and Supplementary Fig. 1). While only a handful of species engaged in biting at more posterior points, in most of those cases bite force peaks at the m2 and then declines further back along the mandible (Supplementary Table 1 and Supplementary Fig. 1). These results suggest that the m1-m2 might represent a boundary between functional regions of the mandible, and lend support to the constrained bite force model (Greaves 1978, 2002; Spencer 1995, 1999) (Fig. 1).

Under the constrained bite force model, during incisor, canine, and premolar biting, the resultant vector of the jaw adductors would pass through the "triangle of support" defined by the bite point and the working and balancing mandible joint forces, creating a region in which bite force increases posteriorly (Fig. 1C). The observed decrease in bite force at the canines does not fit this pattern, however, but this could be the result of a combination of biomechanical and behavioral constraints. For example, because canines are the longest teeth, bats may have experienced a greater stretching of the jaw adductors during canine biting; while we adjusted the distance between the bite plates to ensure a constant gape angle at the biting surface, this might still cause a greater jaw gape (which would result in greater adductor stretching and lower bite force; Herring and Herring 1974; Dumont and Herrel 2003; Santana 2016). Additionally, it is possible that bats refrain from biting the bite force meter at maximum force with their canines to avoid tooth damage, because sharp tooth tips are more prone to breaking when in contact with a hard surface (e.g., Fenton et al. 1998).

During molar biting, the constrained model predicts that the jaw adductor resultant vector would be repositioned toward the working side of the mandible (e.g., via asymmetric muscle activation; Fig. 1B) to avoid tension in the balancing joint, thereby allowing maximum bite force production (Spencer 1998, 1999; Greaves 2002). Our results (i.e., maximum bite forces being commonly located at the m1/m2) are consistent with this proposed mechanism and with previous studies that have demonstrated that bats produce maximum bite forces at the molars when biting unilaterally (Santana and Dumont 2009). Bite force then decreases posterior to the point of maximum bite force in most species; this pattern is consistent with the predicted results of the constrained model and conflicts with the unconstrained model (Fig. 1). Based on the constrained model, the posterior decrease in bite force is possibly the result of tension in the balancing jaw joint during biting, which can no longer be compensated by differential muscle activation (Figs. 1C and 3, and Supplementary Fig. 1).

Based on how bite force changes along the tooth row, we classified species in the dataset into two groups: (1) anterior bite force species (ant-m1-BF; $n = 14$), in which the greatest bite force along the tooth row is at the premolars or at the m1 with the premolars having the second greatest bite force, and (2) posterior bite force species (post-m1-BF; $n = 16$), which includes taxa in which the greatest bite force along the tooth row is posterior to the m1 (i.e., m2 or m3) or at the m1 with more posterior molars having the second greatest bite force (Fig. 3). For species missing bite force data for the m2 (Supplementary Table 1), we classified the species based on the ratio of the premolar bite force to the m1 bite force; species with similar premolar and m1 bite forces were classified as ant-m1-BF, and species with relatively small premolar bite forces were classified as post-m1-BF.

Dietary specialization seems to be associated with bite these force groups; most ant-m1-BF species in our dataset (12 of 14) feed on arthropod and/or vertebrate prey, whereas most post-m1-BF species (12 of 16) feed on plant resources (fruit or nectar). For animalivores, a greater bite force at more anterior teeth may provide an advantage while capturing and killing prey. Conversely, a greater bite force at the molars could confer plant-eating species with advantages during thorough mastication of fruit pulp and/or unilateral molar biting behaviors required to bite into tough fruit (Dumont 1999; Dumont et al. 2009; Santana and Dumont 2009). Additional data on how these bats use specific teeth to

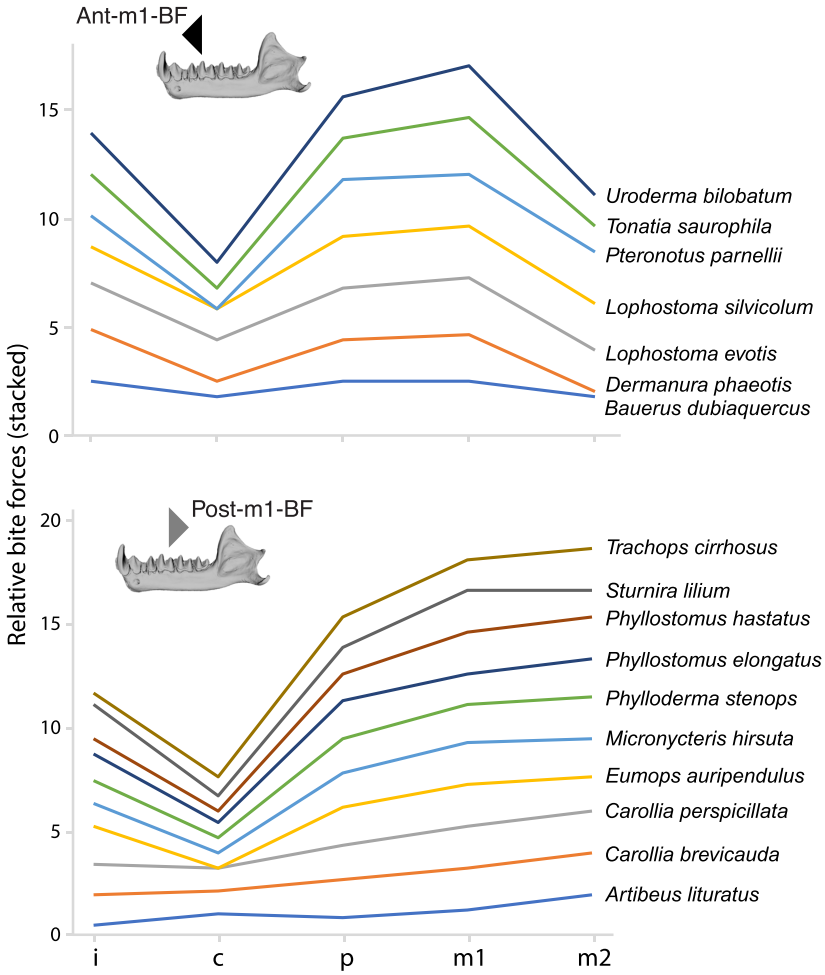

Fig. 3 Relative bite forces (stacked) along the tooth row (i: incisors, c: canine, p: premolars, m1: first molar, m2: second molar) for bat species within the anterior bite force (ant-m1-BF) group (top graph) and posterior bite force (post-m1-BF) group (bottom graph). See text for how these groups were defined. Bite forces were standardized by dividing the results at each tooth by the maximum bite force at any tooth, and then results for each species were stacked (i.e., summed at each tooth position) to facilitate visualization. For instance, *Uroderma bilobatum* and *Trachops cirrhosus* do not have the greatest bite forces but are simply the last species to be stacked. This figure only includes species with recorded bite force data for m2; see Supplementary Figure 1 and Table 1 for bite force data for other species.

consume and process food items would help clarify the relationship between diet and bite force patterns.

What is the relationship between the point of maximum bite force along the tooth row, tooth, and mandible morphology?

Among all the mandibular traits analyzed (Fig. 2, Table 1, Supplementary Table 2), the cross-sectional shape of the mandible body at the m1 is most strongly correlated with interspecific differences in the position of maximum bite force along the tooth row (ant-m1-BF versus post-m1-BF). This trend seems to be primarily driven by variation in mandibular body height (Table 1); species with taller mandibular bodies at the m1, and therefore lower width:height ratios, tend to have more anteriorly positioned maximum bite forces (Fig. 4). Taller mandibular bodies should confer greater resistance to loading in the dorsoventral plane (Hylander 1979; Therrien 2005; Therrien et al. 2016), which would be advantageous when biting into food items with the forceful bites produced in this region. While more information is needed about how width:height ratios vary along the mandible in relation to measured bite force (e.g., Therrien 2005), as well as how internal mandible anatomy (e.g., cortical bone thickness) varies across bats, our results suggest that modeling mandibles as beams to estimate their force profiles could be a promising approach when *in vivo* measurements are not feasible (e.g., in fossil taxa, Brannick and Wilson 2020).

The occlusal area of the ultimate premolar is the only dental trait that was significantly correlated with the position (ant-m1-BF versus post-m1-BF) of maximum bite force (Table 1). Specifically, species with more an-

Table 1 Statistical results of phylogenetic ANOVAs testing the relationship between bite force patterns (anterior-m1-BF, posterior-m1-BF, see text) and morphological measurements of the mandible and teeth

Measurements	*F*-stat	*p*-value	r^2
Mandible			
Mandible length (1)	0.567	0.458	0.021
p to condyle (2)	1.100	0.304	0.040
m1 to condyle (3)	2.952	0.097	0.099
m2 to condyle (4)	2.434	0.130	0.083
m3 to condyle (5)	0.148	0.703	0.005
Coronoid height (6)	0.941	0.341	0.034
Condyle to coronoid (7)	0.068	0.796	0.003
Condyle to angular (8)	0.052	0.821	0.002
Mandible body width (9)	0.912	0.348	0.033
Mandible body height (10)	**11.117**	**0.002**	**0.292**
Mandible body width:height (9/10)	**5.658**	**0.025**	**0.173**
Mandible width:length (at condyle) (11/1)	0.008	0.930	0.000
Mandible width:length (at m1) (12/1)	2.871	0.102	0.096
Teeth			
Total tooth area	0.066	0.799	0.002
p area/tooth row area	**8.813**	**0.006**	**0.246**
m1 area/tooth row area	1.468	0.236	0.052
m2 area/tooth row area	1.510	0.230	0.053
m3 area/tooth row area	1.234	0.276	0.044
Tooth row width:length	0.879	0.357	0.032

Models were run using phylogenetic generalized least squares regression. Numbers in parentheses correspond to the measurement numbers in Fig. 2. Unless specified, measurements were size-standardized by dividing them by the geometric mean of five mandible metrics (measurements 1, 7, 8, 9, and 10 in Fig. 2). Bold font highlights statistical significance at $\alpha = 0.05$. m, molar; p, ultimate premolar.

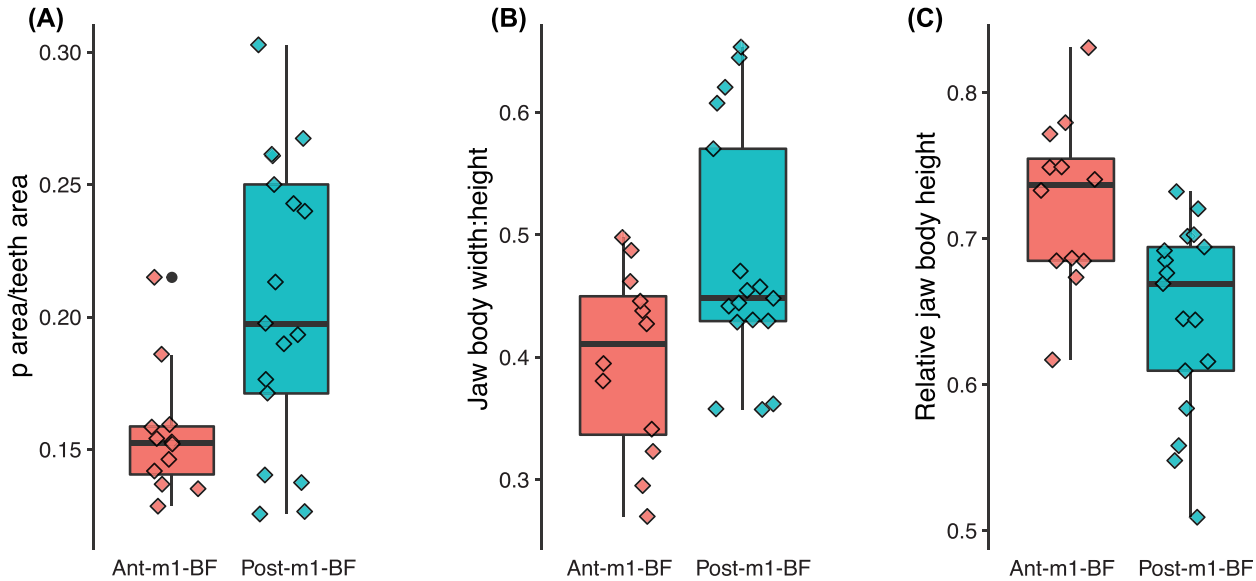

Fig. 4 Box-and-whisker plots for three traits that exhibit a strong relationship with the position of the maximum bite force along the tooth row (ant-m1-BF: species with greatest bite forces at the premolars or at the m1; post-m1-BF species with greatest bite force posterior to the m1; see text for more details). The premolar (p) area is the product of the premolar length and width, which is standardized by dividing by the sum of all measured tooth areas.

teriorly positioned bite forces tend to have smaller ultimate premolars (Fig. 4) with relatively thin, sharp cusps. As the majority of these species are animalivorous, this premolar morphology coupled with higher anterior bite forces is consistent with the role of these teeth in grasping, puncturing, and killing prey (e.g., Freeman 1992; Santana et al. 2011), as well as unique roost-excavating behaviors with the front teeth in two species (*Lophostoma;* Dechmann et al. 2009). Conversely, the ultimate premolars of post-m1-BF species—which are primarily frugivorous or omnivorous—tend to be larger and more molariform in shape. These taxa may be adapted for more posteriorly oriented maximum bite forces because of their strong reliance on molar mastication for digestion of fruit pulp (Dumont 1999; Wagner et al. 2015).

Interestingly, the aforementioned traits (i.e., cross-sectional mandible body shape, premolar area) only show a strong relationship with maximum bite force position in relation to the m1 (i.e., ant-m1-BF versus post-m1-BF). In our second set of comparative analyses, we used the position of maximum bite force relative to mandible length (i.e., distance from the condyle to the tooth with maximum bite force, divided by mandible length), and these analyses did not yield significant results for the cross-sectional mandible body shape or premolar area (Supplementary Table 2). We interpret this discrepancy between these sets of results as supportive evidence for the m1 being a boundary between functional regions of the mandible, with taxa adapting to having more anteriorly oriented or posteriorly oriented bite forces relative to the m1 based on their functional demands.

Surprisingly, no other mandible or tooth measurement—including those related to tooth position along the mandible—was associated with bite force trends along the tooth row (Table 1); the location of the m1 along the mandible was positively related to greater bite forces, but this relationship was weak and not significant (Supplementary Table 2). Previous comparative studies across more distantly related mammal species (e.g., primates, artiodactyls, and carnivorans) found the morphology of the masticatory apparatus and tooth arrangement to be consistent with the constrained model of bite force production that is supported by our data. For example, molars appear to be contained within Region II, presumably because it is the optimal location for powerful chewing teeth (Greaves 1978, 1983, 1985; Biknevicius et al. 1996; Spencer 1999). With the m1 likely representing a boundary between functional regions in our sample of species, this is likely the case in bats as well. Spencer (1999) and Greaves (2000) posited that no mammal has teeth in Region III because biting in this area would inevitably load the working side jaw joint in tension. However, we see a decline in bite force anterior to the edentulous region of the mandible (e.g., at the m2 in ant-m1-BF species), indicating that bats may experience some jaw joint tension when biting with the most posterior molars. A more comprehensive and in-depth study of mandible comparative morphology and biomechanics is needed to define if and where regions of bite force exist in bats. This is becoming increasingly feasible with new datasets detailing 3D mandible musculature (Santana 2018) and skull morphology (Shi et al. 2018; Arbour et al. 2019), although feeding kinematics and electromyography studies are still sorely needed to inform these analyses. Nevertheless, our results suggest additional factors underlie bite force variation along the tooth row, and a greater complexity of mechanisms that could explain the position of teeth at mechanically advantageous positions along the mandible.

How could bite force–morphology relationships relate to the developmental processes controlling tooth formation?

To start addressing this question, we evaluate our results in the context of a pre-existing dataset on tooth morphological development recently published by some of us (Sadier et al. 2021). This dataset included embryonic series of several of the same species (*Artibeus jamaicensis, Carollia perspicillata, Glossophaga soricina, Uroderma bilobatum*), as well as congeners of species (*Pteronotus quadridens, A. phaeotis*) in our dataset, and span the two bite force groups (ant-m1-BF, post-m1-BF) used in our analyses (Fig. 2).

We focused on assessing if the sequence of development and relative size of different teeth across species is consistent with the patterns of bite force along the tooth row described above, particularly the role of the m1 as a boundary between functional regions of the mandible. We find that the teeth that exhibit the highest bite force in most of the species compared—the ultimate premolar and the m1—are the first teeth to develop during ontogeny. This intriguing finding suggests there was selection for developmental mechanisms that position these teeth first at a mechanically advantageous location. Subsequently, the development of these teeth can affect the pace of formation of other molariform teeth (Sadier et al. 2021).

A more careful examination of the successive formation of molariform teeth during development could further explain our findings. Some species in the post-m1-BF group (e.g., omnivore *C. perspicillata* and frugivore *A. jamaicensis*; Sadier et al. 2021) are characterized by loss of the adult p3 at early stages of development and formation of the m2 and m3 (when present) at later developmental stages when compared to species in the

ant-m1-BF group. Therefore, maximum bite forces at the m2 or m3 in these species is associated with several events of developmental origin: (1) reduction of the premolar number anterior to the m1; (2) size reduction of m2 and m3; and (3) delayed formation of m2 and m3 (Sadier et al. 2021). Altogether, this indicates that tooth loss—in addition to the timing of tooth formation—might also be under selection to form molars at mechanically advantageous positions. This idea is also supported by the variable presence of the m3, both among species (e.g., m3 is lost in *Dermanura phaeotis*) and within species (e.g., *D. watsoni*) and in mammals in general. The decline in bite force posterior to the m2 observed in species for which these data were available (Supplementary Figure 1) highlights the lower functional utility these most posterior molars may have in terms of applying forces to food items, which could be a contributing factor to their eventual evolutionary loss.

Finally, we compared the relative size of different molariform teeth (width: length) at different stages of development among the species examined in Sadier et al. (2021). We found that, compared to other species, short-faced, post-m1-BF frugivores like *A. jamaicensis* exhibit a much larger m1 than m2 during development, which is reminiscent of molar proportions in the adults. Conversely, insectivorous and omnivorous post-m1-BF species like *C. perspicillata* (which have relatively longer mandibles than short-faced bats) exhibit little difference in the relative sizes of developing molariform teeth. These results emphasize the importance of the m1 both functionally and as the initiator of the molar row during development (as initially shown by Kavanagh et al. 2007), and more generally that the order by which teeth develop could potentially be linked to dietary functional requirements and specialization in mandible morphology (e.g., mandible length).

Conclusion

Altogether, our results highlight the advantages and challenges associated with using naturally diverse organisms for integrative studies of biological diversity. In comparison to rodents, which are commonly used as model organisms for studying mammals, many bats often maintain an ancestral tribosphenic molar morphology and lack highly derived dental and mandibular traits. Further, bats have experienced an extraordinary adaptive radiation into a wide range of dietary niches, allowing for detailed comparative analyses associated with shifts in diet. Finally, recent studies in bats have established protocols to quantify morphology and performance, and there are growing tools available for studying bat development. Thus, we advocate for bats as a promising system to fully explore the links among morphology, biomechanics, and development.

Supplementary data

Supplementary Data available at *ICB* online.

Acknowledgments

We thank Drs Lara Ferry and Tim Higham for inviting us to participate in the symposium "Integrating ecology and biomechanics to investigate patterns of phenotypic diversity: evolution, development, and functional traits." We also thank Dr Elizabeth Dumont for the discussion of initial ideas related to bite force variation along the tooth row, and for lending equipment for collection of the bite force data at early stages of the study. Dr Nancy Simmons and Marisa Surovy facilitated access to specimens in the mammal collection at the American Museum of Natural History. Johnny Murillo provided field assistance in Venezuela, and data collection in Belize was made possible thanks to a field trip organized by Drs Brock Fenton and Nancy Simmons, and participating colleagues.

Funding

This work was supported by the National Science Foundation [grant numbers 2017738 to S.E.S., 2017803 to K.E.S.].

Data availability

The data underlying this article are available in the Electronic Supplementary Data

References

Arbour JH, Curtis AA, Santana SE. 2019. Signatures of echolocation and dietary ecology in the adaptive evolution of skull shape in bats. Nat Commun 10:2036.

Biknevicius AR, Van Valkenburgh B, Gittleman JL. 1996. Design for killing: craniodental adaptations of predators. In: Carnivore behavior, ecology, and evolution New York: Cornell University Press. p. 393–428.

Brannick AL, Wilson GP. 2020. New specimens of the late Cretaceous metatherian *Eodelphis* and the evolution of hard-object feeding in the Stagodontidae. J Mamm Evol 27:1–16.

Catón J, Tucker AS. 2009. Current knowledge of tooth development: patterning and mineralization of the murine dentition. J Anat 214:502–15.

Christiansen P, Wroe S. 2007. Bite forces and evolutionary adaptations to feeding ecology in carnivores. Ecology 88:347–58.

Crompton A. 1971. The origin of tribosphenic molar. Early mammals: zoological journal of the linnean society. 50:65–87.

Dechmann DKN, Santana SE, Dumont ER. 2009. Roost making in bats—adaptations for excavating active termite nests. J Mammal 90:1461–8.

Drummond AJ, Suchard MA, Xie D, Rambaut A. 2012. Bayesian phylogenetics with BEAUti and the BEAST 1.7. Mol Biol Evol 29:1969–73.
Dumont ER, Dávalos LM, Goldberg A, Santana SE, Rex K, Voigt CC. 2012. Morphological innovation, diversification and invasion of a new adaptive zone. Proc R Soc B Biol Sci 279:1797–805.
Dumont ER, Herrel A, Medellín RA, Vargas-Contreras JA, Santana SE. 2009. Built to bite: cranial design and function in the wrinkle-faced bat. J Zool 279:329–37.
Dumont ER, Herrel A. 2003. The effects of gape angle and bite point on bite force in bats. J Exp Biol 206:2117–23.
Dumont ER, Piccirillo J, Grosse IR. 2005. Finite-element analysis of biting behavior and bone stress in the facial skeletons of bats. Anat Rec Part A 283:319–30.
Dumont ER. 1999. The effect of food hardness on feeding behaviour in Frugivorous bats (Phyllostomidae): an experimental study. J Zool 248:219–29.
Evans A, Wilson G, Fortelius M, Jernvall J. 2007. High-level similarity of dentitions in carnivorans and rodents. Nature 445:78–81.
Fenton MB, Waterman JM, Roth JD, Lopez E, Fienberg SE. 1998. Tooth breakage and diet: a comparison of bats and carnivorans. J Zool 246:83–8.
Freeman P. 1992. Canine teeth of bats (Microchiroptera): size, shape and role in crack propagation. Biol J Linn Soc 45:97–115.
Freeman PW. 1998. Form, function, and evolution in skulls and teeth of bats. In: Kunz TH, (ed.) Bat biology and conservation Washington, DC: Smithsonian Institution Press. p. 140–56.
Greaves W. 2002. Modeling the distance between the molar tooth rows in mammals. Can J Zool 80:388–93.
Greaves WS. 1978. The mandible lever system in ungulates: a new model. J Zool 184:271–85.
Greaves WS. 1983. A functional analysis of carnassial biting. Biol J Linn Soc 20:353–63.
Greaves WS. 1985. The generalized carnivore jaw. Zool J Linn Soc 85:267–74.
Greaves WS. 2000. Location of the vector of mandible muscle force in mammals. J Morphol 243:293–9.
Grossnickle DM, Weaver LN, Jäger KRK, Schultz JA. 2022. The evolution of anteriorly directed molar occlusion in mammals. Zool J Linn Soc 194:349–65.
Herrel A, Podos J, Huber SK, Hendry AP. 2005. Bite performance and morphology in a population of Darwin's finches: implications for the evolution of beak shape. Funct Ecol 19:43–8.
Herrel A, Spithoven L, Van Damme R, De Vree F. 1999. Sexual dimorphism of head size in *Gallotia galloti*: testing the niche divergence hypothesis by functional analyses. Funct Ecol 13:289–97.
Herring SW, Herring SE. 1974. The superficial masseter and gape in mammals. Am Nat 108:561–76.
Hiiemäe KM, Ardran GM. 1968. A cinefluorographic study of mandibular movement during feeding in the rat (*Rattus norvegicus*). J Zool 154:139–54.
Hunter JP, Jernvall J. 1995. The hypocone as a key innovation in mammalian evolution. Proc Natl Acad Sci 92:10718–22.
Hylander WL. 1979. The functional significance of primate mandibular form. J Morphol 160:223–39.
Kavanagh K, Evans A, Jernvall J. 2007. Predicting evolutionary patterns of mammalian teeth from development. Nature 449:427–32.
Luo Z-X. 2007. Transformation and diversification in early mammal evolution. Nature 450:1011–9.
Martin T, Jäger KRK, Plogschties T, Schwermann AH, Brinkkötter JJ, Schultz JA. 2020. Molar diversity and functional adaptations in Mesozoic mammals. In: Martin T, Koenigswald Wv, (eds.) Mammalian teeth—form and function Munich: Verlag. p. 187–214.
Moustakas JE, Smith KK, Hlusko LJ. 2011. Evolution and development of the mammalian dentition: insights from the marsupial *Monodelphis domestica*. Dev Dyn 240:232–9.
Orme D, Freckleton R, Thomas G, Petzoldt T, Fritz S, Isaac N, Pearse W. 2018. CAPER: comparative analysis of phylogenetics and evolution in R, Methods Ecol Evol 3:145–151.
Patterson B. 1956. Early Cretaceous mammals and the evolution of mammalian molar teeth. Fieldiana-Geology 13:1–105.
Pineda-Munoz S, Lazagabaster IA, Alroy J, Evans AR. 2016. Inferring diet from dental morphology in terrestrial mammals. Methods Ecol Evol 1–11.
Sadier AA, Anthwal N, Krause AL, Dessalles R, Bentolila L, Haase R, Nieves N, Santana S, Sears K. 2021. Growth rate as a modulator of tooth patterning during adaptive radiations affiliations. BioRx. https://doi.org/10.1101/2021.12.05.471324.
Salomies L, Eymann J, Ollonen J, Khan I, Di-Poï N. 2021. The developmental origins of heterodonty and acrodonty as revealed by reptile dentitions. Sci Adv 7:1–14.
Santana SE, Dumont ER, Davis JL. 2010. Mechanics of bite force production and its relationship to diet in bats. Funct Ecol 24:776–84.
Santana SE, Dumont ER. 2009. Connecting behaviour and performance: the evolution of biting behaviour and bite performance in bats. J Evol Biol 22:2131–45.
Santana SE, Geipel I, Dumont ER, Kalka MB, Kalko EKV. 2011. All you can eat: high performance capacity and plasticity in the common big-eared bat, *Micronycteris microtis* (Chiroptera: Phyllostomidae). PLoS One 6:e28584.
Santana SE, Grosse IR, Dumont ER. 2012. Dietary hardness, loading behavior, and the evolution of skull form in bats. Evolution 66:2587–98.
Santana SE. 2016. Quantifying the effect of gape and morphology on bite force: biomechanical modeling and *in vivo* measurements in bats. Funct Ecol 30:557–65.
Santana SE. 2018. Comparative anatomy of bat mandible musculature via diffusible iodine-based contrast-enhanced computed tomography. Anat Rec 301:267–78.
Schultz JA, Martin T. 2014. Function of pretribosphenic and tribosphenic mammalian molars inferred from 3D animation. Naturwissenschaften 101:771–81.
Shi JJ, Westeen EP, Rabosky DL. 2018. Digitizing extant bat diversity: an open-access repository of 3D μCT-scanned skulls for research and education. PLoS One 13:1–13.
Simmons NB, Cirranello AL. 2022. Bat species of the world: a taxonomic and geographic database https://batnames.org (01 March 2022, date last accessed).
Spencer MA. 1995. Masticatory system configuration and diet in anthropoid primates [dissertation]. [State University of New York (NY)]: Stony Brook.

Spencer MA. 1998. Force production in the primate masticatory system: electromyographic tests of biomechanical hypotheses. J Hum Evol 34:25–54.

Spencer MA. 1999. Constraints on masticatory system evolution in anthropoid primates. Am J Phys Anthropol 108: 483–506.

Therrien F, Quinney A, Tanaka K, Zelenitsky DK. 2016. Accuracy of mandibular force profiles for bite force estimation and feeding behavior reconstruction in extant and extinct carnivorans. J Exp Biol 23:3738–374.

Therrien F. 2005. Mandibular force profiles of extant carnivorans and implications for the feeding behaviour of extinct predators. J Zool 267:249–70.

Tucker A, Sharpe P. 2004. The cutting-edge of mammalian development; how the embryo makes teeth. Nat Rev Genet 5:499–508.

Upham N, Esselstyn J, Jetz W. 2019. Inferring the mammal tree: species-level sets of phylogenies for questions in ecology, evolution, and conservation, PLoS Biol 17:e3000494.

Wagner I, Ganzhorn JU, Kalko EK V, Tschapka M. 2015. Cheating on the mutualistic contract: nutritional gain through seed predation in the frugivorous bat *Chiroderma villosum* (Phyllostomidae). J Exp Biol 218:1016–21.

Wakamatsu Y, Egawa S, Terashita Y, Kawasaki H, Tamura K, Suzuki K. 2019. Homeobox code model of heterodont tooth in mammals revised. Sci Rep 9: 1–13.